Cartilage and bone cells do not participate in skeletal regeneration in *Ambystoma mexicanum* limbs

CrossMark

Catherine D. McCusker [a,*], Carlos Diaz-Castillo [b], Julian Sosnik [c], Anne Q. Phan [d], David M. Gardiner [b]

[a] Department of Biology, University of Massachusetts Boston, MA 02125, USA
[b] Department of Developmental and Cell Biology, University of California at Irvine, CA 92602, USA
[c] Department of Interdisciplinary Engineering, Wentworth Institute of Technology, Boston, MA 02115, USA
[d] Department of Cellular and Molecular Medicine, University of California San Diego, CA 92093, USA

ARTICLE INFO

ABSTRACT

The Mexican Axolotl is one of the few tetrapod species that is capable of regenerating complete skeletal elements in injured adult limbs. Whether the skeleton (bone and cartilage) plays a role in the patterning and contribution to the skeletal regenerate is currently unresolved. We tested the induction of pattern formation, the effect on cell proliferation, and contributions of skeletal tissues (cartilage, bone, and periosteum) to the regenerating axolotl limb. We found that bone tissue grafts from transgenic donors expressing GFP fail to induce pattern formation and do not contribute to the newly regenerated skeleton. Periosteum tissue grafts, on the other hand, have both of these activities. These observations reveal that skeletal tissue does not contribute to the regeneration of skeletal elements; rather, these structures are patterned by and derived from cells of non-skeletal connective tissue origin.

© 2016 Elsevier Inc. All rights reserved.

1. Introduction

The development and regeneration of many biological structures is dependent on interactions between mesenchymal and epithelial tissue-layers. Signaling feedback loops between these tissues result in the induction of organ fields, which often are temporally and spatially restricted. In both developing and regenerating systems, the mesenchymal component is responsible for imposing regional (or positional) specificity (Cairns and Saunders, 1954; Endo et al., 2004; Muneoka et al., 1986; Saunders et al., 1959). For example, if foot mesenchyme is juxtaposed with wing epithelium in chicken embryos, scales and claw structures form (Cairns and Saunders, 1954; Saunders et al., 1959). Similarly, if mature dermis is grafted from the tail to the forelimb of an adult salamander and a regenerative response is induced, the result is the formation of tail-like structures (Glade, 1963). Thus, the positional cues provided by the mesenchyme play an essential role in patterning the developing organ.

During embryogenesis, the mesenchymal component of these interactions is derived from either the mesoderm or the neural crest (Le Lièvre and Le Douarin, 1975; Noden, 1986). The mesenchyme of the regenerating adult salamander limb, known as the limb blastema, is composed of many cell-types that are also derived from mesodermal or ectodermal embryological origins (Kragl et al., 2009; Nacu et al., 2013). Studies on adult amphibians and mammals have shown that the mesenchymal cells that provide positional cues originate from the mature connective tissues (Chang et al., 2002; Endo et al., 2004; Kragl et al., 2009; Muneoka et al., 1986; Nacu et al., 2013; Wu et al., 2013). Other cell types such as muscle, Schwann, and epidermal cells do not retain positional memory but respond to positional cues from the cells in the connective tissue (Kragl et al., 2009; Muneoka et al., 1986; Nacu et al., 2013). Interestingly, these positionally-naïve cell-types arise from the same embryological origins as the cells that retain positional memory, revealing that it is not a default property of all cells from mesodermal or ectodermal lineage.

Moreover, at this time it is not entirely clear whether cells in all of the connective tissues retain positional memory and provide other tissues with positional cues. For example, the skeletal tissue has evaded our investigations on positional information, and studies to date have yielded contradictory results (reviewed in McCusker et al. (2015)). Part of this confusion lies in the variation in the different aspects of the experimental methodologies that, we later discovered, can drastically effect the outcome without elucidating whether this property is present in the skeletal tissue or not. For example, one test of whether a tissue retains positional

* Corresponding author.
E-mail address: Catherine.mccusker@umb.edu (C.D. McCusker).

information lies in its ability to induce the formation of new pattern (that results in the generation of ectopic structures) when confronted with cells with differing positional information (Endo et al., 2004). Some of the experiments testing this property were conducted on the humerus skeletal element, and because no ectopic structures formed upon 180° rotation of the humerus, it was concluded that this tissue did not have positional information (Carlson, 1975; Goss, 1956; Wigmore and Holder, 1985). However, it was later discovered that the positional information in the internal limb structures is asymmetrically distributed along the proximal/distal limb axis (Gardiner and Bryant, 1989), and consequently these previous surgical manipulations would not be predicted to induce ectopic structures even if this tissue retained positional information. Other experimental differences, such as the age and size of the experimental animals, and whether or not periosteal tissue was included with the grafted tissues, also could underlie the discrepancies among the previous studies (Carlson, 1975; Eggert, 1966; Goss, 1956, 1958; Kragl et al., 2009; Muneoka et al., 1986; Wallace et al., 1974).

Thus, the initial purpose of the current study was to elucidate whether skeletal tissue (bone/cartilage) retains positional information by testing its ability to induce the formation of new limb structures when confronted with cells with differing positional information using the Accessory Limb Model (ALM) (Endo et al., 2004). The ALM is a gain-of-function assay that is based on the induction of ectopic blastemas and supernumerary limb regenerates upon grafting tissue into an innervated wound site on the limb (Endo et al., 2004; McCusker and Gardiner, 2013). The ALM has a number of advantages over the classical amputation-based assay in studying positional confrontations between different tissues. The ALM surgery does not result in the excessive bleeding and trauma that is associated with amputation that makes it more difficult to control how the graft and host tissues heal. In addition ALM assays confer the possibility of targeted positional confrontations, not accessible in amputated regenerates. Both ALM and amputation blastemas are equivalent at the cellular and molecular levels of analysis (Satoh et al., 2007). Lastly, the ALM provides a simplified system to study the essential molecular and cellular requirements during each stage of the regenerative response including the contribution of specific cell types that control the formation of new pattern.

We performed our analysis on ALM surgeries with grafts of the ulna tissue from "young" (6.5 cm snout-to-tail tip larval) or "old" (25 cm snout-to-tail tip sexually mature) animals, or the peri-ulna tissue from "old" animals. We found that the periosteal tissue had robust pattern-inducting properties, being able to induce the formation of ectopic growths with complex pattern, while ulna (without the periosteum) tissue (regardless of age) had little to no pattern-inducing activity. The inductive properties of the periostium are dependent, in part, on the presence of intact Heparin Sulfate chains because cleavage of these chains in the grafted tissue reduces the complexity of the pattern that form in the ectopic limbs. We additionally observed that periosteal tissue is capable of stimulating a more robust cell proliferation response when compared to bone or cartilage. This result reveals that not all connective tissues retain (or communicate) positional memory to induce the formation of new pattern in the regenerate.

Lastly, we found that periosteal cells contribute to a variety of connective tissues (skeletal and non-skeletal) in the regenerating limb. Surprisingly, the skeletal tissue cells did not contribute to any tissue in the limb regenerate. This observation suggests that the regenerated skeleton is derived completely of non-skeletal connective tissue cell origin, including the periosteum. These findings are an important step to understand which cell types contribute to the regenerated skeletal structures and the cellular and molecular basis of pattering during an endogenous regenerative response.

2. Results

2.1. Skeletal and periosteal tissues have different pattern-inducing properties

Previous experiments that were aimed at determining the pattern-inducing capacity of skeletal tissue yielded varied results depending greatly on whether periosteal tissue was excluded or not, as well as on the age/size of the animals that were used. Altogether, the studies suggested that skeletal tissue from young animals have pattern-inducing properties (Gardiner and Bryant, 1989; Wallace et al., 1974), while the pattern-inducing capacity becomes restricted to the periosteal tissue in older animals (Maden and Wallace, 1975; Muneoka et al., 1986; Wallace et al., 1974). Additionally, age related differences have been observed in the developmental origins of limb muscle tissues (Tanaka, 2016). We hypothesized that there are age related changes in the pattern-inducing capacity of the skeletal tissue, and thus we directly tested this idea. It was previously shown that the ulna has posterior positional information (Gardiner and Bryant, 1989). In contrast, the humerus and radius do not have posterior information (Gardiner and Bryant, 1989). Thus, we tested the ability of skeletal ulna tissues (skeletal and periosteum) from animals of different ages to induce the formation of new limb structures when grafted into an anterior-located ALM host site. The grafted tissues were dissected from the ulna of young (6.5 cm) and old (25 cm) transgenic animals expressing GFP and grafted into 7–10 cm white-axolotl host wounds (Fig. 1, Table 1). Live images were obtained of all of the ectopic blastemas with skeletal grafts throughout the experiment, and the presence of the grafted tissue was evaluated by observing the presence of GFP-positive cells (Fig. 1A). The limbs were harvested 7-weeks post-grafting, and whole mount cartilage staining was performed to assess the pattern of supernumerary skeletal elements (Fig. 1B).

To control that minimal contaminating tissue was included with the grafted tissue, we characterized the morphology of intact and dissected skeletal tissue from young animals (6.5 cm) and older animals (25 cm–sexually mature) (see Fig. 1 in Ref. McCusker et al. (submitted for publication)). Intact ulna, or dissected ulna or peri-ulna tissues were sectioned transversally and stained with hematoxylin, eosin, and alcian blue. The dissected ulna and peri-ulna tissues used for grafting (see Fig. 1A′, B′ and B″ in Ref. McCusker et al. (submitted for publication·)) showed morphological characteristics that were similar to the ones observed in the intact tissues. It is noteworthy that the dissected ulna tissue from the young animals (cartilaginous) retained a few contaminating perichondrial cells, while the dissected ulna from the larger animals (ossified) had no observable contaminating periosteal cells. This difference is likely due to the greater technical difficulty of dissecting off the perichondrial tissue from the young ulnas because of their smaller size.

We observed marked differences in the pattern-inducing capacity of ulna and peri-ulna tissue grafts when assayed in the ALM. Ulna grafts (i.e. bone) from old animals had the least pattern-inducing capacity, where only single nodules of cartilage were present in the wound site (63%) (Fig. 1, Table 1). We suspect that in some cases this single nodule is the remnant of the original grafted tissue rather than the formation of new cartilage because in many cases the GFP fluorescence in the live images was spatially coincident with the location of the nodule observed in the whole mount staining. Young ulna tissue grafts (i.e. cartilage) also had minimal pattern-inducing capacity. Similar to the old ulna grafts, the majority of young ulna grafts that resulted in ectopic cartilage had only a single nodule of cartilage (52%). However, a few of the young ulna grafts resulted in the formation of multi-segmented skeletal elements (19%). While the young ulna tissue appears to
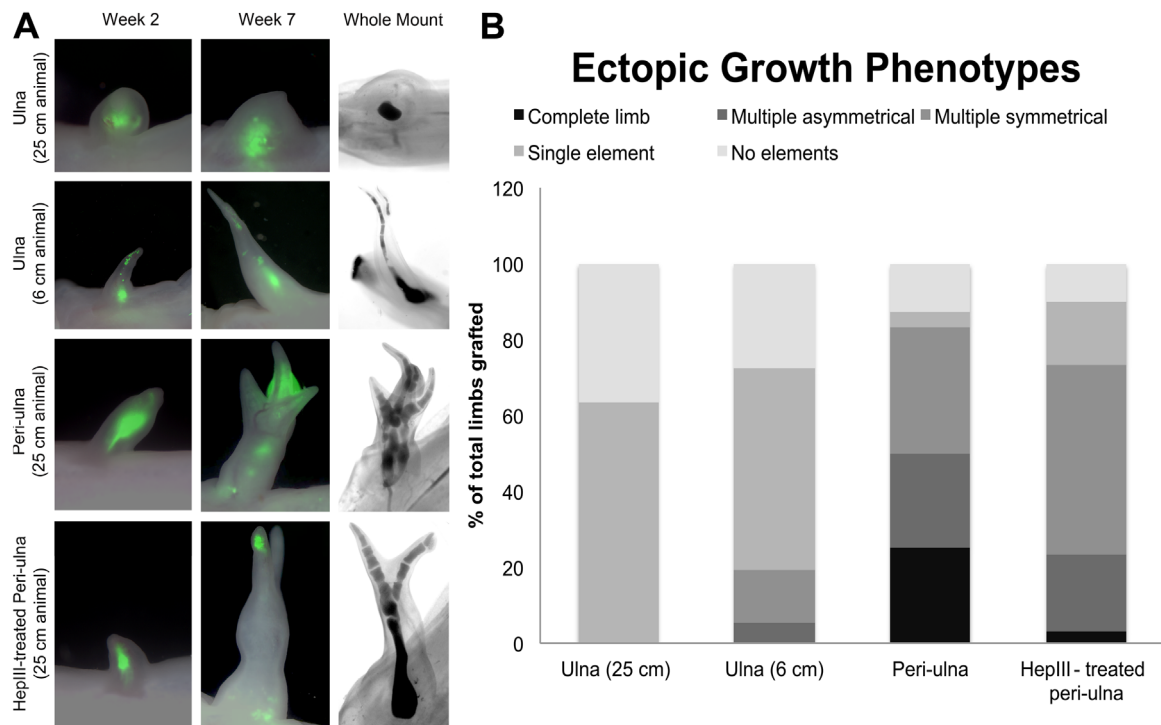
Fig. 1. Periosteal tissue induction of supernumerary limb structures is inhibited by HS depletion. Skeletal and peri-skeletal tissues from the ulna of either 6 cm or 25 cm animals were grafted into limbs with anterior-located wounds with a deviated nerve. (A) Fluorescent images of GFP+ (grafted population) overlaid on bright field images show the presence of the grafted population in the ectopic blastema two and seven weeks post-grafting (left). Whole mount Victoria Blue staining was performed to analyze the formation of ectopic skeletal structures in wound sites at 7-weeks post-grafting. Images are of the most complete growth response observed from grafts of ulna (25 cm animal), ulna (6 cm animal), peri-ulna (25 cm animal), or Heparinase III-treated peri-ulna (25 cm animal). (B) The percentage of the total number of grafted ALM limbs that resulted in the formation of no elements, a single element, multiple-symmetrical elements, multiple-asymmetrical elements, or a complete limb as determined by whole mount cartilage staining as described in McCusker and Gardiner (2013). The number of ALM limbs analyzed for each graft type was as follows: ulna 25 cm animal (N=33), ulna 6 cm animal (N=36), Heparinase III treated peri-ulna (N=30), peri-ulna (N=24) (see Table 1 for more details).

Table 1

Ectopic graft induction phenotypes from ulna and peri-ulna grafts into an ALM.

Graft type	Total ALMs performed	ALMs Counted[a]	No element[b]	Single element[b]	Multiple symmetrical elements[b]	Multiple asymmetrical elements[b]	Complete limb[b]
Ulna (25 cm)	34	33	12 (36.4%)	21 (63.6%)	0 (0%)	0 (0%)	0 (0%)
Ulna (6 cm)	37	36	10 (27.8%)	19 (52.8%)	5 (13.9%)	2 (5.6%)	0 (0%)
Peri-ulna	26	24	3 (12.5%)	1 (4.1%)	8 (33.3%)	6 (25%)	6 (25%)
HepIII- treated peri-ulna	30	30	3 (10%)	5 (16.6%)	15 (50%)	6 (20%)	1 (3.3%)

[a] ALMs that did not have GFP+ grafted cells visible 3 weeks post grafting were excluded from the analysis.

[b] Number of ALMs with phenotype (% of total ALMs).

have a slightly higher pattern-inducing capacity than the old tissue, we suspect that this difference may be caused by contaminating perichondrial tissue in the young ulna graft (as discussed above). In comparison to the ulna grafts from old and young animals, the peri-ulna grafts (from old animals), had a robust pattern-inducing activity. Most of the grafts lead to ectopic growths (87%), and 50% of the total number of the grafts led to complete supernumerary or hypomorphic limbs. In summary, the periosteal grafts had a robust pattern-inducing activity, while the cartilage and bone grafts from young and old animals, respectively, had minimal pattern-inducing capacity.

2.2. The pattern-inducing activity of periosteal tissue was reduced upon removal of heparan sulfate chains

It was reported recently that the extracellular matrix (ECM) has pattern-inducing properties that are mediated through heparan sulfate chains (Phan et al., 2015). We reasoned that the cells that retain positional memory communicate this information (at least

in part) to the surrounding environment by expressing specific heparan sulfates on the cell surface and in the ECM. Thus, we hypothesized that the depletion of heparan sulfate from periosteal tissue would inhibit its inductive properties. To test this hypothesis, we depleted the heparan sulfate in the periosteal tissue grafts by treating them with heparinase-III, which cleaves the heparan sulfate chains (HS) on the HSPGs (Pojasek et al., 2000). We quantified the amount of HS cleavage by western blot and immunofluorescence, along with the percent of tunnel positive peri-ulna cells with increasing duration of incubation with heparinase-III to determine the optimal length of the treatment (Supplemental Fig. 1). We found that HS cleavage was detectable by three hours of treatment, while we did not see an increase in tunnel staining until four hours of treatment (Supplemental Fig. 1). Thus, we treated the peri-ulna tissue grafts for three hours with either heparinase-III or PBS prior to grafting into the ALM. Heparinase III treatment of the peri-ulna grafts resulted in a decrease in the complexity of the ectopic growths that they elicited in the ALM assay. In contrast to the peri-ulna grafts, only one of the 30

heparinase-III treated grafts resulted in the formation of a completed limb in the ALM (Fig. 1B, Table 1). We did not extend our analysis to observe whether HS depletion also negatively affected the induction of structures from bone or cartilage grafts because these grafts exhibited minimal inductive activity.

2.3. Differential activation of non-autonomous cell proliferation in ulna and peri-ulna grafted ALM blastemas

According to the Polar Coordinate Model of regeneration, when cells with differing positional information interact in a regeneration-permissive environment an intercalary response is elicited, which generates new cells with the missing positional information (Bryant et al., 1981; French et al., 1976). Thus, since peri-ulna grafts resulted in ectopic formations with more complicated pattern than ulna grafts in the ALM assay, we predicted that peri-ulna grafts would also elicit a greater proliferative response. To test this idea, we measured the EdU labeling index in ALM blastemas, 10 days after grafting the ulna or peri-ulna tissue from a 25 cm animal. These blastemas corresponded to mid-bud (MB) to late bud (LB) blastemas that would form in response to limb amputation, and we chose this stage because it was prior to the point at which there was an obvious difference in the shape and size of the grafted blastemas. We observed that both the ulna and peri-ulna grafted ALM blastema mesenchyme exhibited an overall increase in proliferation compared to the adjacent, uninjured tissues. At this early stage of regeneration, the labeling index was significantly greater (130% greater) in the host mesenchyme of the peri-ulna grafts compared to ulna grafted ALM blastemas (26% to 20% positively labeled, respectively) (Fig. 2A). It is likely that this difference in proliferation increases at later time points because at these stages the peri-ulna ALMs continue, while the ulna-grafted ALMs cease to grow. Thus, the periosteal grafts induced a greater non-autonomous proliferative response and resulted in the induction of more complex pattern; whereas, the bone grafts resulted in a lesser proliferative response and induced no (or simple) limb pattern.

Proliferation in ulna versus peri-ulna ALM blastemas
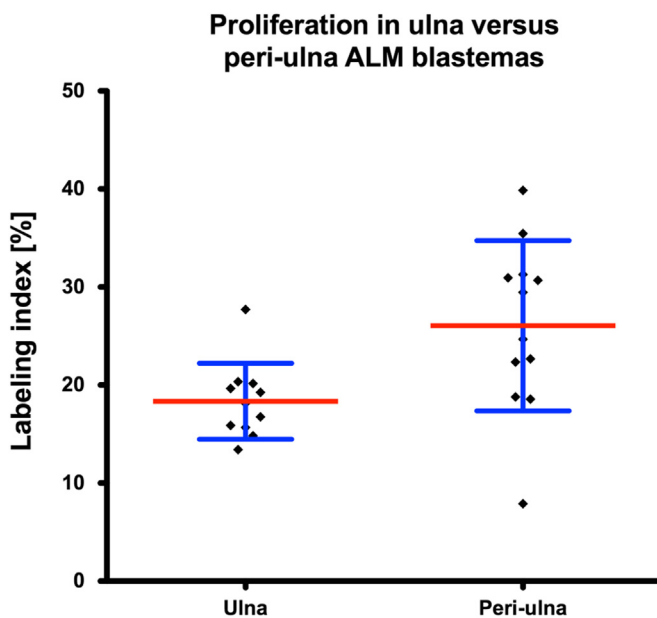
Fig. 2. Differential induction of tissue growth in ulna and peri-ulna grafted blastemas. Scatter plot of the average labeling index of the host cells in ALM blastemas with Ulna (N=10) or peri-ulna (N=12) grafts. The labeling index was determined by dividing the number of EdU+ cells, by the total number of cells in a specific population and multiplying by 100. Ulna vs peri-ulna: degrees of freedom (df)=18; t=2.653; P=0.0162.

It is important to clarify that the current proliferation analyses were performed without distinguishing the progenitor cell types in the blastema mesenchyme. Thus, we are unable to determine whether there are differences in proliferation between "pattern forming" progenitors (from the connective tissue) and "pattern following" (e.g. muscle and Schwan cell progenitors) in the ulna and peri-ulna grafted ALM blastemas.

2.4. Periosteal grafts contributed to connective and skeletal tissues in the limb regenerate, but skeletal grafts did not

Cells in the limb have differing abilities to contribute to the tissues of the regenerate (Kragl et al., 2009). Some cell types are very lineage restricted, only contributing to the same tissue type of their origin from the limb stump. Muscle and Schwann cells are examples of these types (Kragl et al., 2009; Nacu et al., 2013). Conversely, cells of connective tissue origin have flexibility in terms of the tissues that they contribute to. For example blastema cells of dermal origin contribute to both connective tissues and the skeletal elements of the regenerated limb (Lheureux, 1983; Kragl et al., 2009; Muneoka et al., 1986). Interestingly, the cell types that retain positional memory (i.e. "pattern forming") exhibit flexibility in the tissues they contribute to, whereas the other cell types that are more restricted do not retain positional memory (i.e. "pattern following"). Based on these previous observations, we predicted that periosteal tissue, which has the ability to induce new limb structure, should contribute to both connective and skeletal tissues in the regenerate. Skeletal tissue, on the other hand, should be restricted to contributing to skeletal tissue only.

To test this hypothesis we grafted these tissues to wounds made in the proximal region (humerus) of the host limb, such that the grafted cells would have the possibility of contributing to the tissues of more distal structures in the regenerate. Thus, to alleviate the potential of inducing proximal/distal positional discontinuities between the graft and host cells, we grafted tissues from the humerus rather than the ulna, as in the previous experiments. After grafting, we observed which tissues in the regenerate the grafted cells contributed to. As we had predicted, cells of periosteal origin were present throughout the regenerate and contributed to a variety of tissues (Figs. 3A–A′, and 3C–G). As had been previously observed with dermal tissue grafts (Kragl et al., 2009), the periosteal grafts contributed to cells in the skeletal elements (Fig. 3C), connective tissues throughout the limb (Fig. 3D–F), and fibroblast-like cells associated with the vasculature (Fig. 3G). Surprisingly, bone grafts had little to no contribution to bone or any other of the tissues in the regenerate (Figs. 3B–B′, and H–I). The majority of the grafted bone cells remained associated with the stump location where they were grafted, yet we sometimes saw a few GFP-positive cells in the regenerated tissues (Fig. 3I). These cells were fibroblast-like and were located in the dermis or other connective tissues. We suspect that these GFP-positive cells correspond to a small number of contaminating periosteal cells that were present in the grafts (see Fig. 1D″ in Ref. McCusker et al. (submitted for publication)).

3. Discussion

3.1. Regeneration of a complete limb requires both "pattern forming" and "pattern following" cells

While it is possible to regenerate much of a limb from cells with positional information (i.e. "pattern forming"), regeneration of a limb with all of the limb tissues requires the contribution of cell-types that do not retain positional information, and thus the ability to form pattern, but respond to cells that do (i.e. "pattern
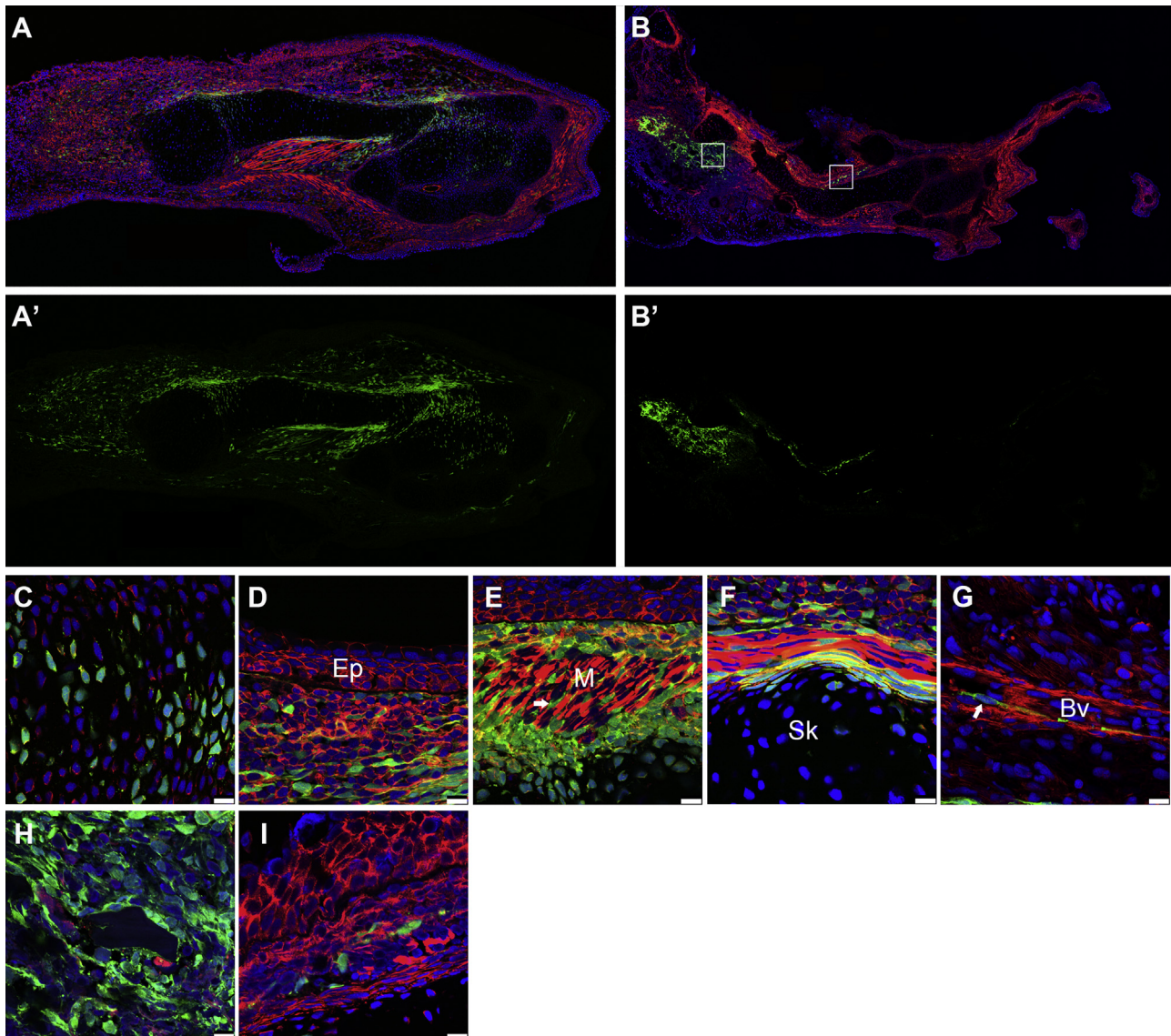
Fig. 3. Contribution of skeletal and periosteal grafts in regenerated limb tissues. (A–A') Confocal image of a transverse section of a regenerated limb that had been grafted with peri-humerus tissue from a transgenic animal expressing GFP. The limb was amputated through the mid-humorous. Note the extensive contribution of GFP positive cells to the regenerated limb structure. (N=7; all 7 regenerates showed extensive GFP+ cell contribution to dermis, periosteum, skeleton, and muscle connective tissue) (A) Fluorescence is of DAPI (blue) and phalloidin-rhodamine (red) staining and GFP (green) positive graft cells or (A') only the GFP positive cells in (A). (B–B') Confocal image of a transverse section of a regenerated limb that had been grafted with humerus tissue from a transgenic animal expressing GFP (white boxes indicate the location of the higher magnification images in H and I). Note that most of the grafted ulna cells do not contribute to the regenerated structures. (N=6; 5 of the 6 had nearly all of GFP+ cells located at the graft site in the stump. A few isolated cells could be seen in the dermis, periosteum, and skeleton in the regenerate (representative image in H). (C–G) Representative fluorescent images of GFP positive cells from the peri-humerus graft contributing to different tissues in the regenerated limb structure in including cartilage (C), dermal cells ("Ep" indicates epidermis) (D), fibroblast-like cells (white arrow) in the muscle tissue ("M" indicates muscle) (E), periosteal tissue ("Sk" indicates skeletal tissue) (F), and fibroblast-like cells (arrow) associated with blood vessels ("BV") (G). Fluorescent channels are as described for (A). (H–I) Fluorescent images were captured of GFP positive cells from the humerus graft in the regenerated limb. (H) GFP positive cells that have remained in the graft site. (I) A small number of GFP positive cells from the humerus graft contribute to the regenerate. White scale bars in C-H are 25 μM in length.

following") (Dunis and Namenwirth, 1977; Holder et al., 1979; Kragl et al., 2009; Nacu et al., 2013). In the current study we have identified the periosteal tissue as "pattern forming cells", based on their ability to induce the formation of new pattern when grafted into a different location on the limb. We have identified that heparan sulfate is at least partially responsible for the pattern-forming activity of periosteal tissue. We additionally found that while skeletal tissue is not a "pattern forming" cell-type in young (cartilage) or old (bone) animals, it also does not appear to be a "pattern following" cell type either since cells derived from this tissues do not contribute to the regenerate (current study; Muneoka et al., 1986). Thus, our results indicate that the skeleton regenerates by a mechanism that is different from the other limb tissues. The skeletal cells at the amputation plane remain localized and eventually integrate with the new skeletal tissues that form from cells of a non-skeletal connective tissue origin; skeletal tissue do not contribute directly to the new bone that is regenerated.

3.2. Regenerated skeletal tissue is derived completely of cells from connective tissue origin

The amputation of boneless amphibian forelimbs results in the regeneration of the skeletal elements distal to the amputation plane (Goss, 1956; Wigmore, 1985), revealing that non-skeletal cells can undergo metaplasia to regenerate skeletal tissue in the limb. Cell lineage studies using dermal-tissue grafts have shown

that cells of dermal origin differentiate into chondrocytes and contribute to the regenerated skeleton (Dunis and Namenwirth, 1977; Kragl et al., 2009). In the current study we have used transgenic animals expressing GFP as a lineage tracer and have found that periosteal tissue shares this ability (Fig. 3C). Similarly, the periostium plays a pivotal role in bone healing and regeneration in mammals, and differentiates into osteoblasts, chondrocytes, osteocytes, and perivascular vessel cells (Zhang et al., 2005; Zreiqat et al., 2014). Additionally, we have discovered that the differentiated skeletal tissue does not contribute to the regenerated skeletal elements (Fig. 3B). This observation is consistent with those reported by Muneoka et al. (1986), who discovered that cartilage grafts had minimal contribution (2%) to the limb blastema using triploid/diploid cell markers. However, this observation differs from the conclusion of Kragl et al. (2009), who observed that grafts of GFP+ skeletal tissue contributed extensively to the regenerated limb structures. Kragl et al. did not specify whether the peri-skeletal tissue was removed from the cartilage prior to grafting into the host limb. From our current results, any adherent peri-skeletal tissues would be expected to contribute to the regenerated limb, and thus the previous observations may have been the results of contaminate peri-skeletal tissue included with the skeletal grafts. Altogether, these results indicate that the regenerated skeletal elements are derived largely or entirely from cells of non-skeletal origin. They also suggest that the non-skeletal connective tissue cells (including dermal and periosteal) are responsible for the patterning and regeneration of the limb skeleton.

It remains unclear as to why skeletal tissue fails to contribute to the regenerate. It is possible that the dense ECM in this tissue provides a physical barrier that prevents mobilization of the cells that would be required in order for them to participate in regeneration. However, in the current study it was apparent that the ECM was degraded enough such that the individual skeletal cells were freed and in contact with cells in the surrounding environment (Fig. 3H). Thus, it is possible that additional genetic or epigenetic barriers prevent the skeletal cells from contributing to the blastema and the regenerated limb structures.

3.3. Is positional memory lost in non-skeletal connective tissue cells when they differentiate into skeletal tissue?

Based on their ability to induce the formation of new pattern, non-skeletal connective tissue cells retain positional memory (current study; Endo et al., 2004). During regeneration however, these cells contribute to skeletal tissue, which we have determined does not have inductive properties. This suggests that they do not retain positional memory, and that non-skeletal connective tissue cells must loose their positional memory when they differentiate into skeletal tissue during regeneration. We suggest that skeletal cells either do not have positional memory, or do not have the ability to communicate their positional information sufficiently to induce new pattern because they are surrounded by a dense extracellular matrix. In this regard, we observed that the bone tissue grafts in contribution study had dramatically different morphology compared to this tissue prior to grafting (Compare Fig. 3H with Fig. 1B′ in Ref. McCusker et al. (submitted for publication)). We observed that the ECM of the grafted bone tissue has mostly disappeared by the time of the analysis (in 6 of 6 grafts), and that the cells appear to be in very close proximity to each other and the host environment. Although we did not determine whether the grafted cells were making direct cell-cell interactions, it appears that the ECM of the skeletal tissue is remodeled sufficiently to release these cells such that they can physically interact with the cells in the surrounding environment (Fig. 3H). Thus, it is unlikely that this is the reason why the bone grafts fail to induce

pattern in the ALM assay, and we interpret this to indicate that these cells do not have positional memory.

Studies on transgenic axolotls with a retinoic-acid responsive element driving GFP expression provide additional support for the hypothesis that skeletal tissue does not retain positional memory (Monaghan and Maden, 2012). Ectopic exposure to retinoic acid reprograms the positional information in the blastema to a more proximal location on the limb (Maden, 1983; McCusker et al., 2014; Niazi et al., 1985). Since only some of the limb cells retain positional information and control the formation of the pattern in the regenerate, it follows that the RA-mediated positional-reprogramming is occurring specifically in those cells. Consistent with this idea, RA-treatment of blastema on RARE-GFP animals resulted in the induction of GFP expression in a subset of cells throughout the blastema and connective tissue dense regions of the uninjured limb (such as the dermis). The exception to this was the skeletal tissues, which were devoid of GFP expression (Monaghan and Maden, 2012). Presumably, ectopic exposure to RA does not activate the RARE-GFP reporter in the skeletal tissue cells because they do not retain positional information.

Together, these observations suggest that non-skeletal connective tissue cells loose memory of their positional identity as they differentiate into skeletal tissue. If so, understanding how this memory is regulated could provide valuable insight into controlling the inductive properties of cells that exhibit aberrant growth in some human diseases, such as cancers.

4. Materials and methods

4.1. Animal husbandry and surgeries

The experiments in this study were performed on Mexican axolotls (Ambystoma mexicanum) that were either spawned at the University of California, Irvine or obtained from the Ambystoma Genetic Stock Center, University of Kentucky. This study was carried out in accordance with the recommendations in the Guide for the Care and Use of Laboratory Animals of the National Institutes of Health. The experimental work was approved by the Institutional Animal Care and Use Committee of the University of California Irvine. For all surgeries, animals were anesthetized using a 0.1% solution of MS222 (Ethyl 3-aminobenzoate methanesulfonate salt, Sigma), pH 7.0.

The Accessory Limb Model (ALM) assay was performed on 7–10 cm (snout-to-tail tip) host animals, similar to the procedure described in (Endo et al., 2004). Briefly, a 2 mm square of full-thickness skin was removed from the anterior region of the host forelimbs, and the severed end of the brachial nerve was deviated to the center of the wound. The wound was allowed to heal for 48 h to develop a wound epithelium prior to grafting the skeletal or periosteal tissues. The wound epithelium was then slit along the ventral edge, and was separated from the underlying tissue to form a pocket for the tissue grafts. The grafted tissues were inserted into the pocket such that roughly one third of the graft was covered with the mature skin surrounding the wound, and the other two thirds of the graft were under the wound epithelium region of the ALM. We have observed in the past that this method of grafting prevents the loss of the grafted tissues prior to the reestablishment of the wound epithelium on the ALM.

Donor tissues were collected from transgenic animals expressing GFP that were either 20–25 cm (snout to tail tip) in length ("old" animals), or 5.5–7 cm ("young" animals). Periosteal tissue was harvested from the large animals by teasing off the thin connective tissue covering from the dissected ulna element using watchmaker's forceps. The periosteal tissue was rinsed with cold Holfreter's solution, and contaminating muscle tissue was

removed. The cartilaginous epiphyseal caps were removed from the ulna diaphysis, which was scrapped to remove any residual peri-ulna tissue. The diaphyseal region was cut longitudinally to expose the central cavity, and the marrow-like cells and leftover periosteal tissues were removed with forceps and a cold Holtfreter's solution rinse. The ulna was harvested from young animals by dissecting the element, removing the epiphyseal caps, and scraping and rinsing off the periosteal tissue from the diaphysis with forceps and cold Holtfreter's solution. Since the diaphysis of the young animals does not have a marrow-like cavity, the element was not further processed before grafting into the host ALM assay. We did not test the perichondreal tissue from the young animals because we were technically unable to dissect this tissue from the ulna without destroying both tissues. The ulna on the small/young animals is very small in size, and is much more fragile because it is not ossified as it is in the older animals (where the periskeletal tissue can be removed fairly easily). Care was taken to perform our analysis using grafts of roughly the same size. The intact ulna tissue of the young animals was the smallest in size compared to the peri-skeletal and bone tissue from the older animals. Thus, we trimmed the size of the donor tissues from the larger animals to be roughly the size of the diaphysis of the ulna from the smaller animals. Images were obtained of the graft site 1, 2, 3, 5, and 7 weeks post-grafting. Grafts that were not visible by GFP fluorescence 3 weeks following the grafting surgery were excluded from the final analyses.

To determine the contribution of periosteal and skeletal tissue in the tissues of the regenerate, the peri-humerus and humerus tissue were harvested from large transgenic GFP animals as described above, and grafted under the wound epithelium of host limbs on white animals (7–10 cm snout to tail tip) whose limbs had been amputated at the mid-humerus level 48 h prior to grafting. The host limbs were harvested once the tissues had differentiated (approximately 5 weeks following the grafting procedure), and the limbs were processed for cryosectioning (periosteal grafts; N=7, and bone grafts: N=6). Limb sections were stained with phalloidin-rhodamine (Life technologies), and mounted in Vectasheild mounting medium with DAPI (Vector labs).

4.2. Heparinase-III treatment

Prior to grafting into the ALM, some of the periosteal grafts were pretreated with either $1 \times$ PBS or heparinase-III from Flavobacterium heparinium (Seikagaku) diluted to 0.001 U/ml in $1 \times$ PBS. The periosteal tissues were incubated with heparinase-III for 3 h at room temperature with gentle agitation. Following treatment, the tissues were washed twice for 15 min with PBS prior to grafting the tissues into the wound site of a 7–10 cm host animal. Control periosteal grafts underwent the same procedure as above except the grafts were incubated in PBS rather than the heparinase-III solution.

4.3. Immunostaining and quantification of cleaved-HSPG signal

Tissue samples were fixed in 4% PFA in $1 \times$ PBS, embedded in OCT compound (Tissue-Tek) and sectioned into 10 µM sections for immunodetection. Immunofluorescence was performed as described in (McCusker and Gardiner, 2013). The heparan sulfate delta epitope was detected using 3G10 (US Biologicals) primary antibody diluted to 1:200 in $1 \times$ PBS-Tween (incubated overnight at 4°C), and Alexa Fluor® 594 conjugated chicken anti-mouse IgG (Life Technologies) secondary antibody diluted to 1:200 in $1 \times$ PBST, and mounted in Vectashield with DAPI (Vector Laboratories). Fluorescent images were obtained using a Leica PL FLUOTAR 40 × / 0.70 objective mounted on a Leica Leitz DMRB Fluorescence microscope, and a Qimaging QIClick-F-M-12 camera controlled by Qimaging QCapture 2.9.13 software. For each time point, three images of three different sections were obtained (n=9 technical replicates for each time point). Fiji software was used to transform the images into binary, the background was set to a threshold of 0.1%, and the area of pixels in each image with signal above the background threshold was quantified.

4.4. Western blot analysis of cleaved heparan sulfate

Following heparinase-III treatment the periosteal tissue samples were extracted directly in $2 \times$ Laemmli buffer with (5%) β-mercaptoethanol and boiled for 5 min. Total protein was loaded onto a 4–20% precast gradient gel (Bio-Rad) and transferred to nitrocellulose membrane (Bio-Rad). Membranes were blocked in 1% (w/v) BSA in $1 \times$ PBST. The heparan sulfate delta epitope was detected using the 3G10 primary antibody diluted to 1:200 in $1 \times$ PBST, the HRP conjugated anti-mouse secondary antibody (GE Healthcare Life Sciences), diluted 1:3000 in $1 \times$ PBST, and ECL Western Blotting System (GE Healthcare Life Sciences). As a loading control, the peroxidase was inactivated using hydrogen peroxide and the membranes were reprobed with the anti-(beta) tubulin antibody (Developmental Studies Hybridoma Bank), diluted to 1:200 in $1 \times$ PBST, and then incubated with HRP conjugated anti-mouse secondary antibody (GE Healthcare Life Sciences) diluted 1:3000 in $1 \times$ PBST. The ECL Western Blotting System (GE Healthcare Life Sciences) was used to detect the immunolabeled protein bands. To quantify the amount of protein in each lane, the developed films were scanned and transformed into 8-bit images using Fiji (Schindelin et al., 2012), and densitometry analysis was performed using the Fiji set of tools to analyze gels.

4.5. Intercalation assay

To determine the amount of cell proliferation occurring in the ALM assay, animals were injected IP with 0.1 µg of Edu 10 days after the ulna or peri-ulna tissue was grafted. The limbs were harvested 2 h after the EdU injection, fixed in 1% PFA for 1 h at room temperature, and prepared for cryosectioning. The cells that had incorporated EdU into the newly synthesized DNA were detected with the Click-it EdU 488 Imaging Kit following the manufacturer's protocol (Invitrogen). The nuclei of all cells were labeled with DAPI. Ectopic blastema tissue sections that had GFP+ cells present (minimum of 3 sections per blastema) were included in the analysis. The labeling indices of the host (GFP−) populations were calculated by determining the ratio of EdU+ cells to the total number of cells in each population and multiplying by 100. The average labeling index of the host tissue was calculated for each individual blastema.

4.6. Whole mount cartilage staining: (Victoria blue protocol)

Whole mount Victoria blue staining was performed as described in Bryant and Iten (1974) on limbs 7-weeks after the tissue engraftment. The presence of Victoria blue stained ectopic cartilage structures in the ALM assay was observed, and each was scored according to the number of skeletal elements that had formed.

4.7. Histology staining and quantification

Sections of whole limbs that were harvested from 6.5 cm and 25 cm animals, or of dissected peri-ulna and ulna tissue from 6.5 cm and 25 cm animals, were analyzed by histology to determine the tissue composition of the graft sources (Supplemental Fig. 1). The tissue sections were stained with Hematoxylin, Eosin Y, and Alcian Blue as described in Lee and Gardiner (2012).

Competing interests

Author contributions

CDM contributed to the conception, design, execution and interpretation of the findings being published, and drafting the article. CDC contributed to the execution, interpretation of findings, and drafting the article. JS contributed to the interpretation and the drafting of the article. AP contributed to the design and drafting of the manuscript. DMG contributed to the conception, design, interpretation of results, and drafting the article.

Funding

Acknowledgements

Appendix A. Supporting information

Supplementary data associated with this article can be found in the online version at http://dx.doi.org/10.1016/j.ydbio.2016.05.032.

References

Bryant, S.V., French, V., Bryant, P.J., 1981. Distal regeneration and symmetry. Science 212, 993–1002.

Bryant, S.V., Iten, L.E., 1974. The regulative ability of the limb regeneration blastema of Notophlhalmus viridescens: Experiments in situ. Wilhelm Roux' Archiv 174, 90–101.

Cairns, J.M., Saunders, J.W., 1954. The influence of embryonic mesoderm on the regional specification of epidermal derivatives in the chick. J. Exp. Zool. 127, 221–248.

Carlson, B.M., 1975. The effects of rotation and positional change of stump tissues upon morphogenesis of the regenerating axolotl limb. Dev. Biol. 47, 269–291.

Chang, H.Y., Chi, J.-T., Dudoit, S., Bondre, C., van de Rijn, M., Botstein, D., Brown, P.O., 2002. Diversity, topographic differentiation, and positional memory in human fibroblasts. Proc. Natl. Acad. Sci. USA 99, 12877–12882.

Dunis, D.A., Namenwirth, M., 1977. Role of grafted skin in regeneration of X-irradiated axolotl limbs. Dev. Biol. 56, 97–109.

Eggert, R.C., 1966. The response of X-irradiated limbs of adult urodeles to autografts of normal cartilage. J. Exp. Zool. 161, 369–389.

Endo, T., Bryant, S.V., Gardiner, D.M., 2004. A stepwise model system for limb regeneration. Dev. Biol. 270, 135–145.

French, V., Bryant, P.J., Bryant, S.V., 1976. Pattern regulation in epimorphic fields. Science 193, 969–981.

Gardiner, D.M., Bryant, S.V., 1989. Organization of positional information in the axolotl limb. J. Exp. Zool. 251, 47–55.

Glade, R.W., 1963. Effects of tail skin, epidermis, and dermis on limb regeneration in Triturus viridescens and Siredon mexicanum. J. Exp. Zool. 152, 169–193.

Goss, R.J., 1956. The relation of bone to the histogenesis of cartilage in regenerating forelimbs and tails of adult Triturus viridescens. J. Morphol. 98, 89–123.

Goss, R.J., 1958. Skeletal regeneration in amphibians. Development 6, 638–644.

Holder, N., Bryant, S.V., Tank, P.W., 1979. Interactions between irradiated and unirradiated tissues during supernumerary limb formation in the newt. J. Exp. Zool. 208, 303–310.

Kragl, M., Knapp, D., Nacu, E., Khattak, S., Maden, M., Epperlein, H.H., Tanaka, E.M., 2009. Cells keep a memory of their tissue origin during axolotl limb regeneration. Nature 460, 60–65.

Le Lièvre, C.S., Le Douarin, N.M., 1975. Mesenchymal derivatives of the neural crest: analysis of chimaeric quail and chick embryos. J. Embryol. Exp. Morphol. 34, 125–154.

Lee, J., Gardiner, D.M., 2012. Regeneration of Limb Joints in the Axolotl (Ambystoma mexicanum). PLoS One 7, e50615.

Lheureux, E., 1983. The origin of tissues in the X-irradiated regenerating limb of the newt Pleurodeles waltlii. Prog. Clin. Biol. Res. 110 (Pt A), 455–465.

Maden, M., 1983. The effect of vitamin A on the regenerating axolotl limb. J. Embryol. Exp. Morphol. 77, 273–295.

Maden, M., Wallace, H., 1975. The origin of limb regenerates from cartilage grafts. Acta Embryol. Exp., 77–86.

McCusker, C., Lehrberg, J., Gardiner, D., 2014. Position-specific induction of ectopic limbs in non-regenerating blastemas on axolotl forelimbs. Regeneration 1, 27–34.

McCusker, C., Bryant, S.V., Gardiner, D.M., 2015. The axolotl limb blastema: cellular and molecular mechanisms driving blastema formation and limb regeneration in tetrapods. Regeneration 2, 54–71.

McCusker, C.D., Gardiner, D.M., 2013. Positional information is reprogrammed in blastema cells of the regenerating limb of the axolotl (Ambystoma mexicanum). PLoS One 8, e77064.

McCusker, C.D., Diaz-Castillo, C., Sosnik, J., Phan, A., Gardiner, D.M., 2016. Histological Characterization of Limb Skeletal Tissue in Larval and Adult Ambystoma Mexicanum, (submitted for publication as Data in Brief).

Monaghan, J.R., Maden, M., 2012. Visualization, of retinoic acid signaling in transgenic axolotls during limb development and regeneration. Dev. Biol. 368, 63–75.

Muneoka, K., Fox, W.F., Bryant, S.V., 1986. Cellular contribution from dermis and cartilage to the regenerating limb blastema in axolotls. Dev. Biol. 116, 256–260.

Nacu, E., Glausch, M., Le, H.Q., Damanik, F.F.R., Schuez, M., Knapp, D., Khattak, S., Richter, T., Tanaka, E.M., 2013. Connective tissue cells, but not muscle cells, are involved in establishing the proximo-distal outcome of limb regeneration in the axolotl. Dev. Stem Cells, 140.

Niazi, I.A., Pescitelli, M.J., Stocum, D.L., 1985. Stage-dependent effects of retinoic acid on regenerating urodele limbs. Wilhelm Roux' Archiv Entwickl. 194, 355–363.

Noden, D.M., 1986. Origins and patterning of craniofacial mesenchymal tissues. J. Craniofacial Genet. Dev. Biol. Suppl. 2, 15–31.

Phan, A.Q., Lee, J., Oei, M., Flath, C., Hwe, C., Mariano, R., Vu, T., Shu, C., Dinh, A., Simkin, J., et al., 2015. Position information in axolotl and mouse limb ECM is mediated via heparan sulfates and FGF during limb regeneration in the Axolotl (Ambystoma mexicanum). Regeneration, 182–201.

Pojasek, K., Shriver, Z., Hu, Y., Sasisekharan, R., 2000. Histidine 295 and histidine 510 are crucial for the enzymatic degradation of heparan sulfate by heparinase III. Biochemistry 39, 4012–4019.

Satoh, A., Gardiner, D.M., Bryant, S.V., Endo, T., 2007. Nerve-induced ectopic limb blastemas in the axolotl are equivalent to amputation-induced blastemas. Dev. Biol. 312, 231–244.

Saunders, J.W., Gasseling, M.T., Cairns, J.M., 1959. The differentiation of prospective thigh mesoderm grafted beneath the apical ectodermal ridge of the wing bud in the chick embryo. Dev. Biol. 1 (3), 281–301.

Schindelin, J., Arganda-Carreras, I., Frise, E., Kaynig, V., Longair, M., Pietzsch, T., Preibisch, S., Rueden, C., Saalfeld, S., Schmid, B., et al., 2012. Fiji: an open-source platform for biological-image analysis. Nat. Methods 9, 676–682.

Tanaka, H.V., Ng, N.C.Y., Yang Yu, Z., Casco-Robles, M.M., Maruo, F., Tsonis, P.A., Chiba, C., 2016. A developmentally regulated switch from stem cells to dedifferentiation for limb muscle regeneration in newts. Nat. Commun. 7, 11069.

Wallace, H., Maden, M., Wallace, B.M., 1974. Participation of cartilage grafts in amphibian limb regeneration. J. Embryol. Exp. Morphol. 32, 391–404.

Wigmore, P., Holder, N., 1985. Regeneration from isolated half limbs in the upper arm of the axolotl. J. Embryol. Exp. Morphol. 89, 333–347.

Wu, Y., Wang, K., Karapetyan, A., Fernando, W.A., Simkin, J., Han, M., Rugg, E.L., Muneoka, K., 2013. Connective tissue fibroblast properties are position-dependent during mouse digit tip regeneration. PLoS One 8, e54764.

Zhang, X., Xie, C., Lin, A., Ito, H., Awad, H., 2005. Periosteal progenitor cell fate in segmental cortical bone graft transplantations: implications for functional tissue engineering. J. Bone Miner. Res. 20 (12), 2124–2137.

Zreiqat, H., Dunstan, C., Rosen, V., 2014. A Tissue Regeneration Approach to Bone and Cartilage Repair. Springer, New York, NY.